

**Metal doped black In₂O₃ for atmospheric pressure CO₂ photothermal reduction
with high efficiency and selectivity**

Yang Yang^{a,b,1,*}, Liqiang Zhang^{b,1}, Jiaxin Wang^a, Hao Song^a, Xiao Zhang^a, Xiang
Gao^{a,b,*}

^aState Key Laboratory of Clean Energy Utilization, Zhejiang University, Hangzhou
310027, PR China

^bInstitute of Carbon Neutrality, Zhejiang University, Hangzhou 310027, PR China

*Corresponding Authors

¹Co-first authors

DFT calculations

Spin-polarized DFT calculations were performed using the Vienna ab initio simulation package (VASP).^{1,2} The generalized gradient approximation proposed by Perdew, Burke, and Ernzerhof (GGA-PBE) is selected for the exchange-correlation potential.³ The pseudo-potential was described by the projector-augmented-wave (PAW) method.⁴ To accurately describe the dispersion interaction, we use DFT-D3 method with Becke-Jonson damping for dispersion correction.⁵ The geometry optimization was performed until the Hellmann–Feynman force on each atom is smaller than 0.02 eV·Å⁻¹. The energy criterion was set to 10⁻⁴ eV in the iterative solution of the Kohn-Sham equation. The Brillouin zone was sampled with 2×2×1 Monkhorst-Pack k-point mesh, and a Gaussian smearing of 0.05 eV was applied to speed up electronic convergence. Based on a computational hydrogen electrode (CHE) model proposed by Nørskov and co-workers,^{6,7} the Gibbs reaction free energy (ΔG) for CO₂ reduction was defined as,

$$\Delta G = \Delta E + \Delta ZPE - T\Delta S$$

where ΔE is the change of electronic energy, ΔZPE is the change of zero point energy, T is the system temperature (298.15 K), ΔS is the change of entropy, respectively. Under the potential of 0 V vs. RHE, the CHE method relates the chemical of proton-

electron pairs ($H^+ + e^-$) as $1/2 H_2$ (g). A vacuum height of 15 Å along the vertical direction was selected to avoid the unwanted interaction between the slab and its period images.

The dimension of the optimized cubic In_2O_3 model consist of 72 O atoms and 48 In atoms, and the $Cu-In_{2-x}O_3$ model consist of 65 O atoms, 48 In atoms and 3 Cu atoms. distributed in three In-O-In tri-layers. In the calculation, the oxygen vacancy near the Cu atom is used as the active site for the $Cu-In_{2-x}O_3$ system, and In is used as the active site for the In_2O_3 system.

1. G. Kresse, J. Hafner, Phys. Rev. 1993, 47, 558.
2. G. Kresse, J. Furthmuller, Phys. Rev. 1996, 54, 11169.
3. J. P. Perdew, K. Burke, Phys., Rev. Lett. 1996, 77, 3865.
4. P. E. Blöchl, Phys. Rev. B 1994, 50, 17953.
5. S. Grimme, S. Ehrlich, L. Goerigk. J. Comput. Chem. 2011, 32, 1456.
6. R. A. Albery, J. Biol. Chem., 1969, 244, 3290-3302.
7. J. Rossmeisl, J. K. Nørskov, C. D. Taylor, M. J. Janik, M. Neurock, J. Phys. Chem. B, 2006, 110, 21833-21839.

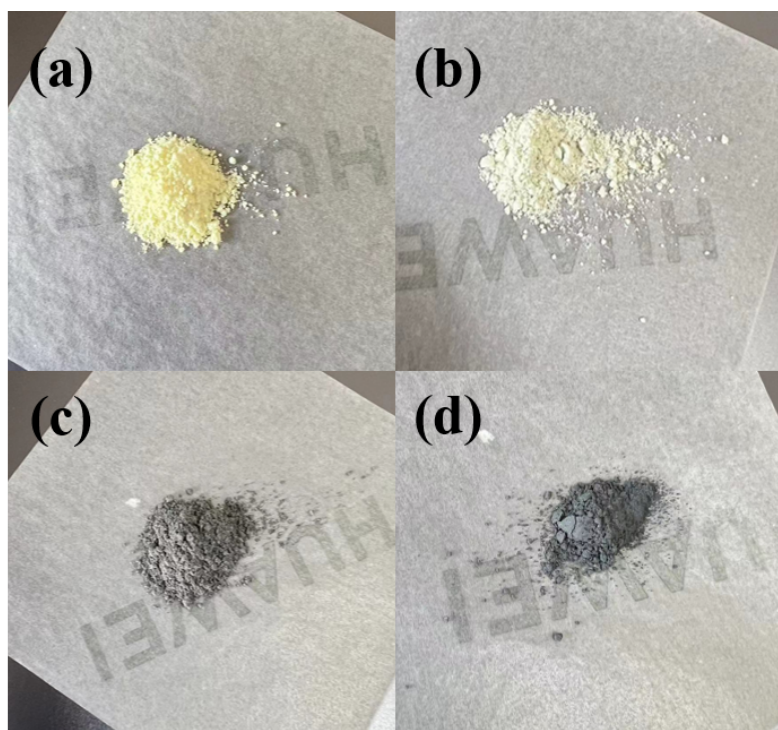


Fig. S1 Digital pictures of $\text{In}_2\text{O}_{3-\text{x}}$ treated with H_2 at (a) 25°C , (b) 200°C , (c) 300°C and (d) 400°C .

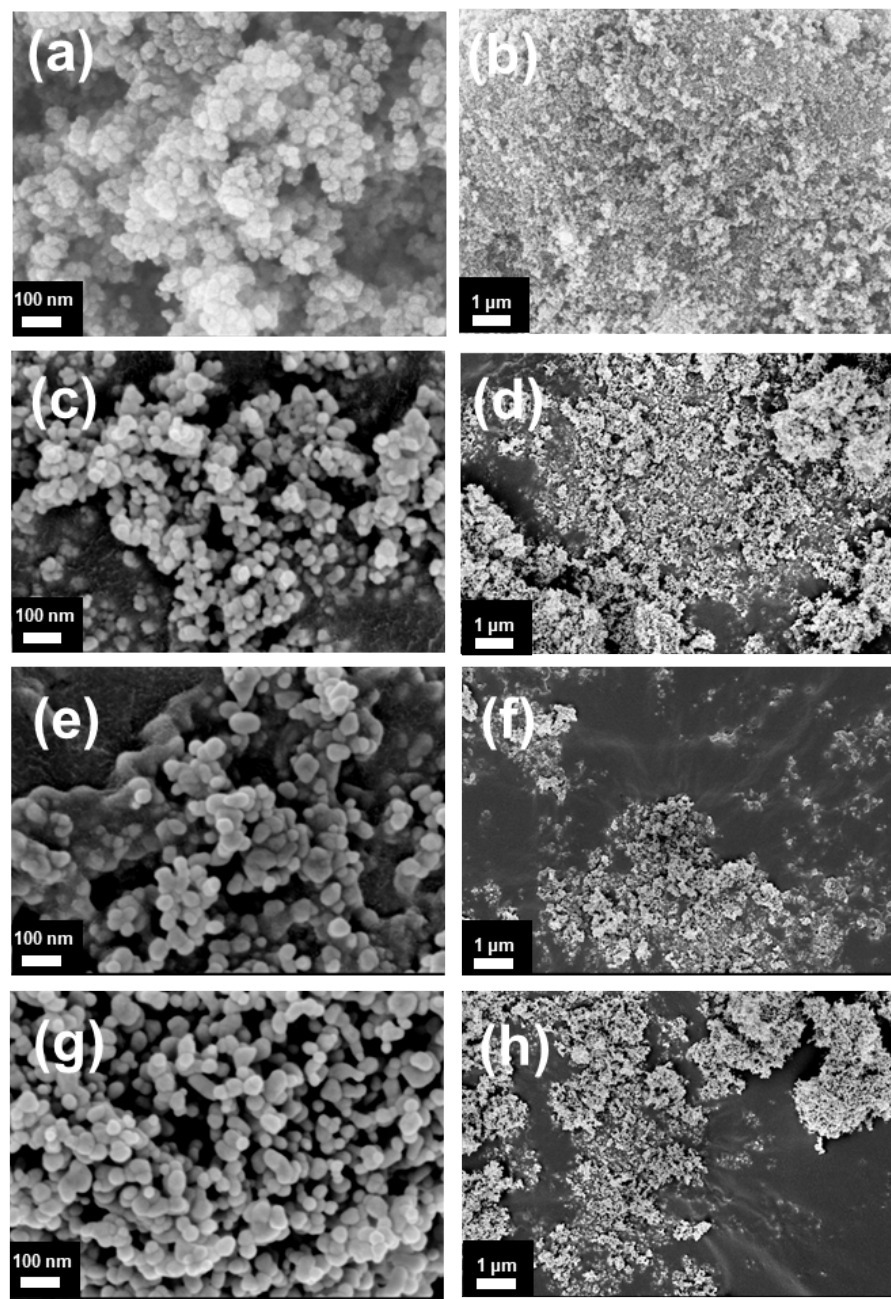


Fig. S2 SEM images of $\text{In}_2\text{O}_{3-\text{x}}$ treated with H_2 at (a-b) 25°C, (c-d) 200°C, (e-f) 300°C and (g-h) 400°C.

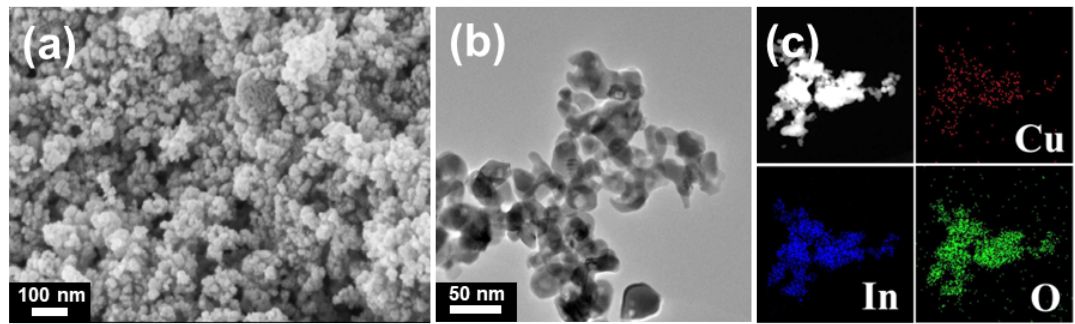


Fig. S3 (a) SEM image of Cu-In₂O_{3-x}. (b) and (c) are TEM and the corresponding mapping images of Cu-In₂O_{3-x}.

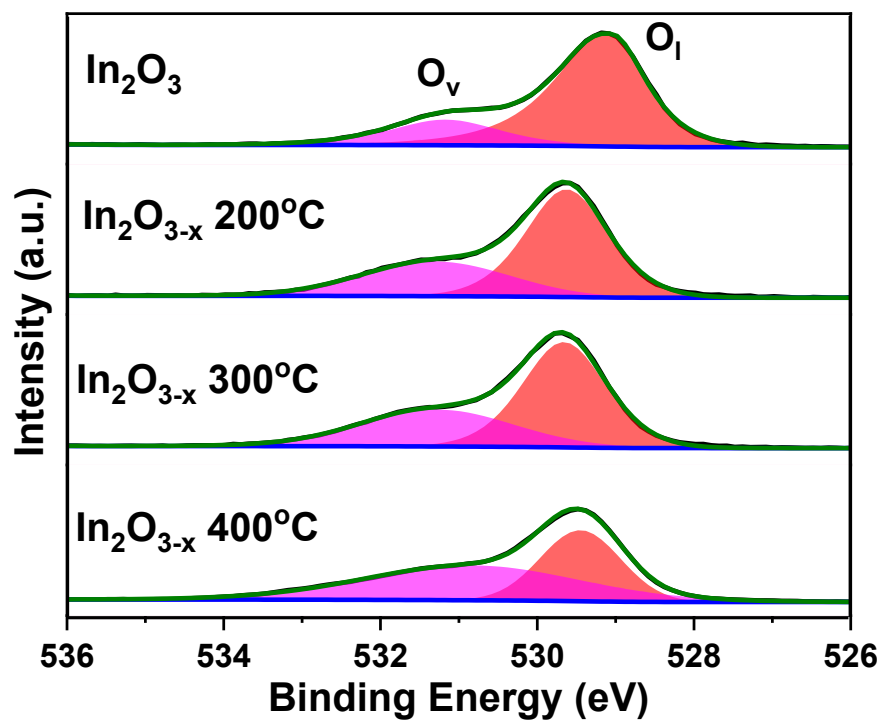


Fig. S4 XPS spectra of O 1s of $\text{In}_2\text{O}_{3-\text{x}}$ treated with H_2 at different temperatures.

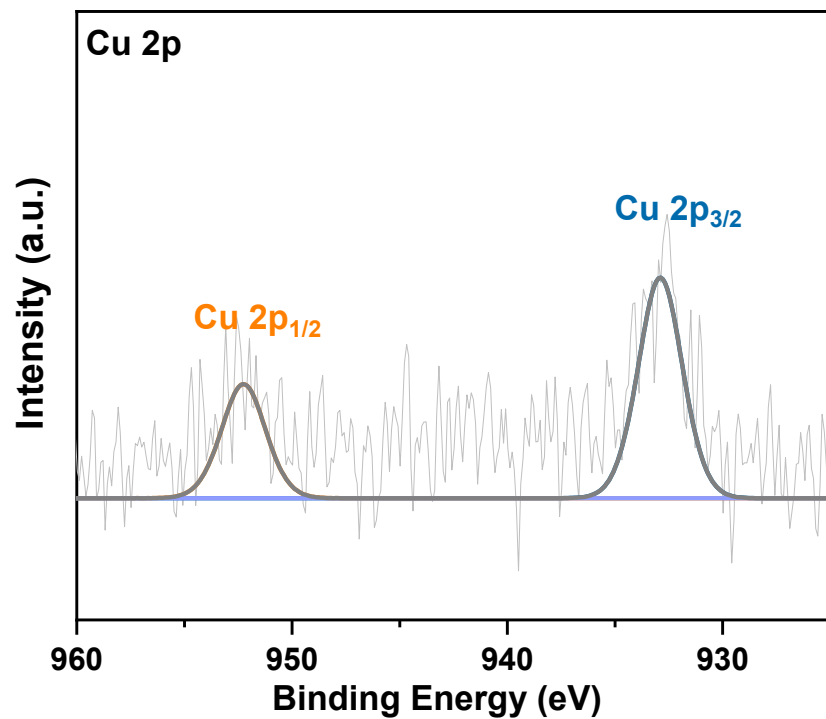


Fig. S5 XPS spectra of Cu 2p of Cu-In₂O_{3-x}.

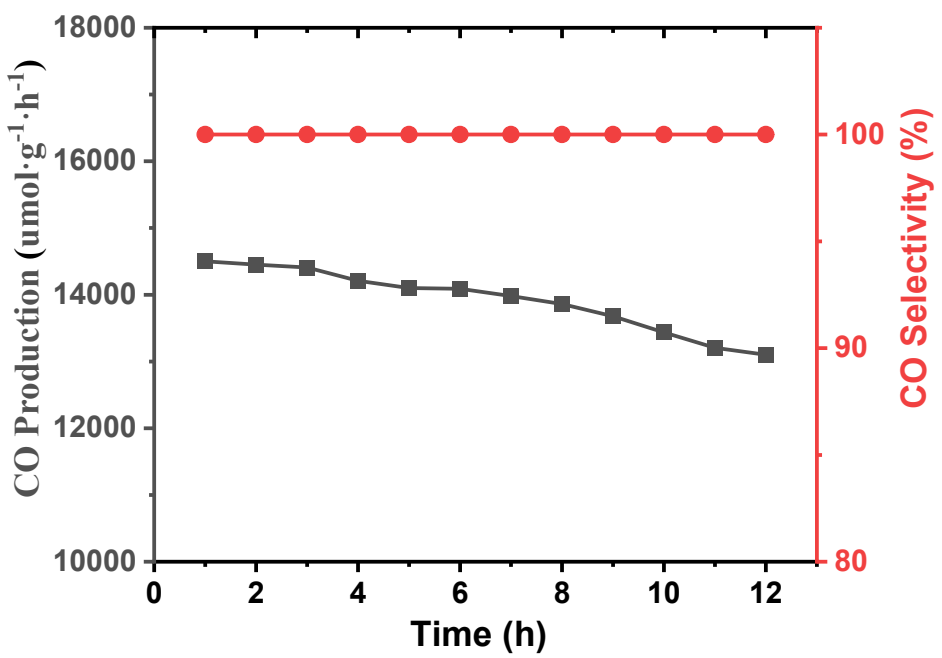


Fig. S6 CO yield and selectivity of Cu-In₂O_{3-x} at 300°C for 12 h.

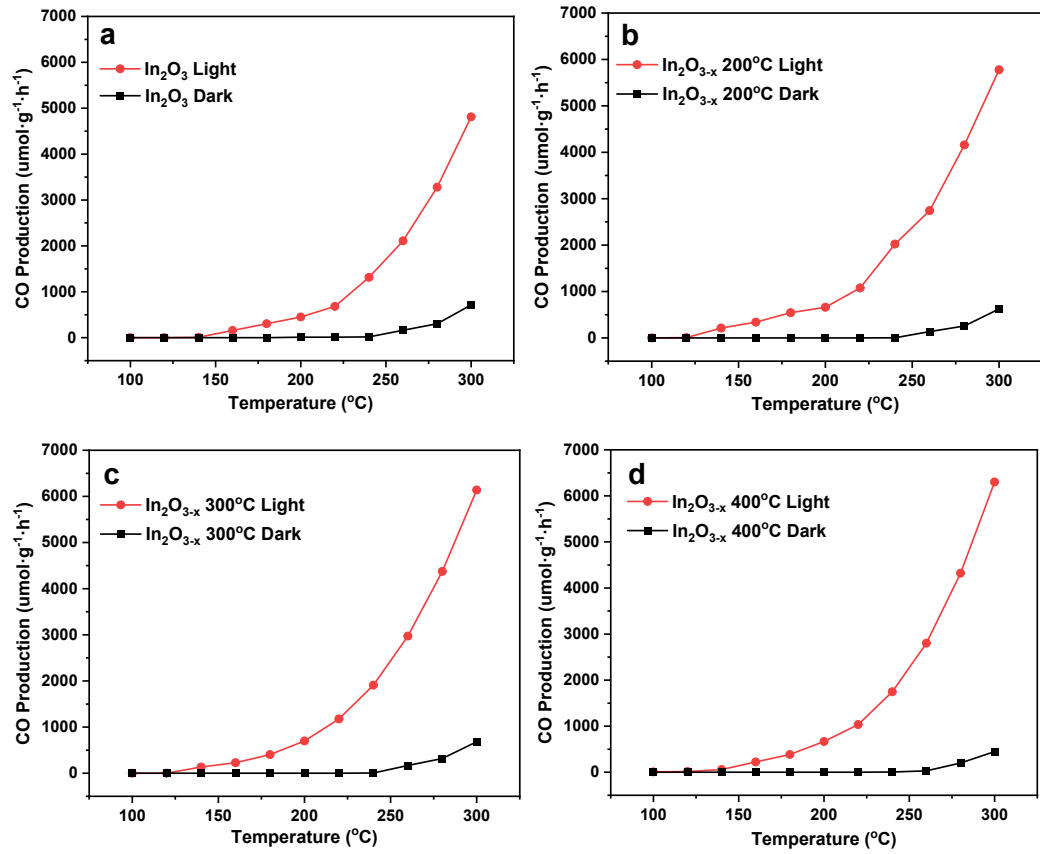


Fig. S7 Comparison of photothermal and thermal catalytic activities of $\text{In}_2\text{O}_{3-\text{x}}$ treated with H_2 at (a) 25 $^{\circ}\text{C}$, (b) 200 $^{\circ}\text{C}$, (c) 300 $^{\circ}\text{C}$, (d) 400 $^{\circ}\text{C}$.

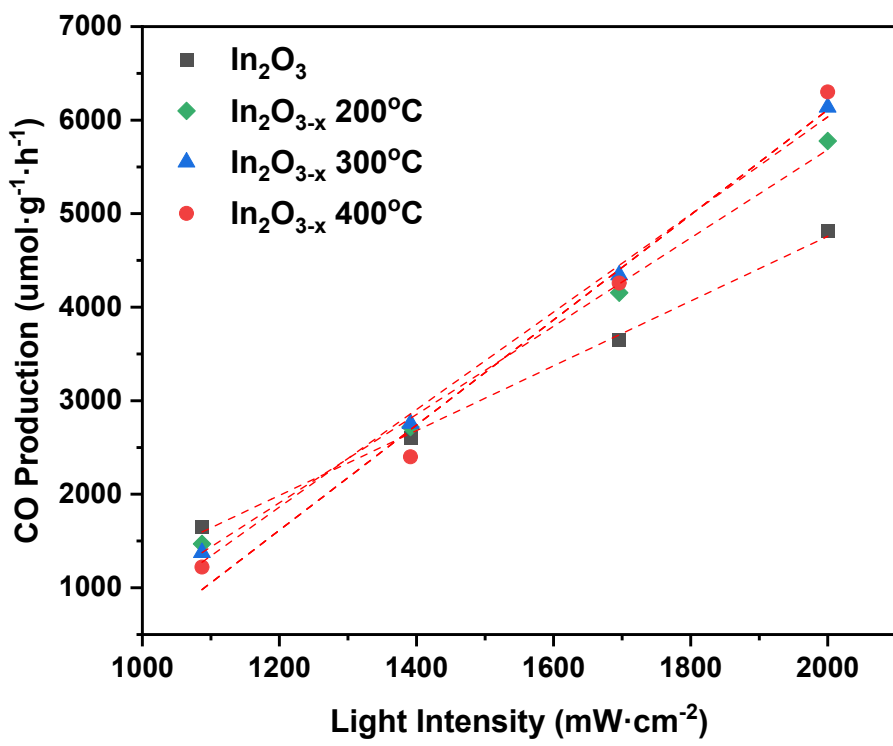


Fig. S8 Photothermal catalytic performance of $\text{In}_2\text{O}_{3-x}$ treated with H_2 at different temperatures at reaction temperature of 300°C.

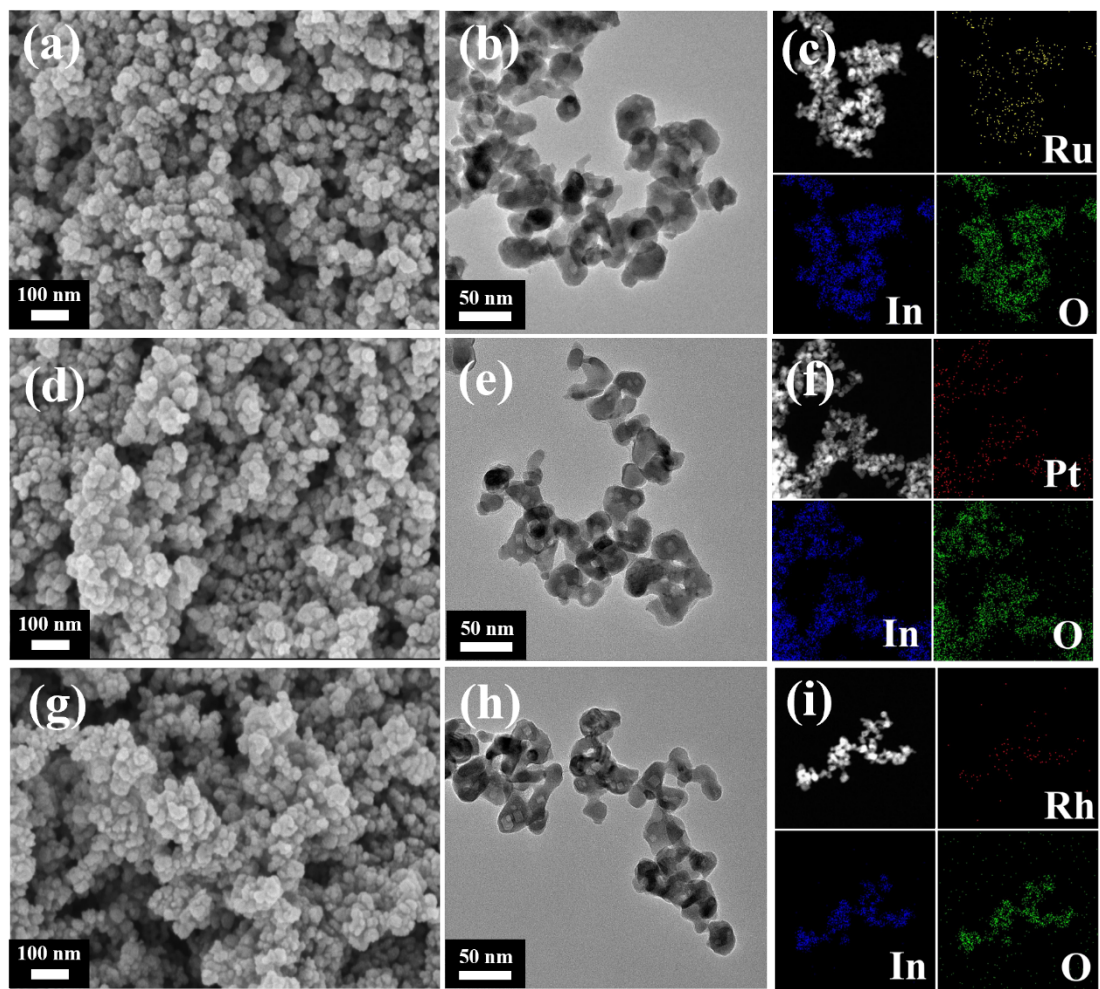


Fig. S9 (a) SEM image of Ru-In₂O_{3-x}, (b) and (c) are TEM and the corresponding mapping images. (d) SEM image of Pt-In₂O_{3-x}, (e) and (f) are TEM and the corresponding mapping images. (g) SEM image of Rh-In₂O_{3-x}, (h) and (i) are TEM and the corresponding mapping images.

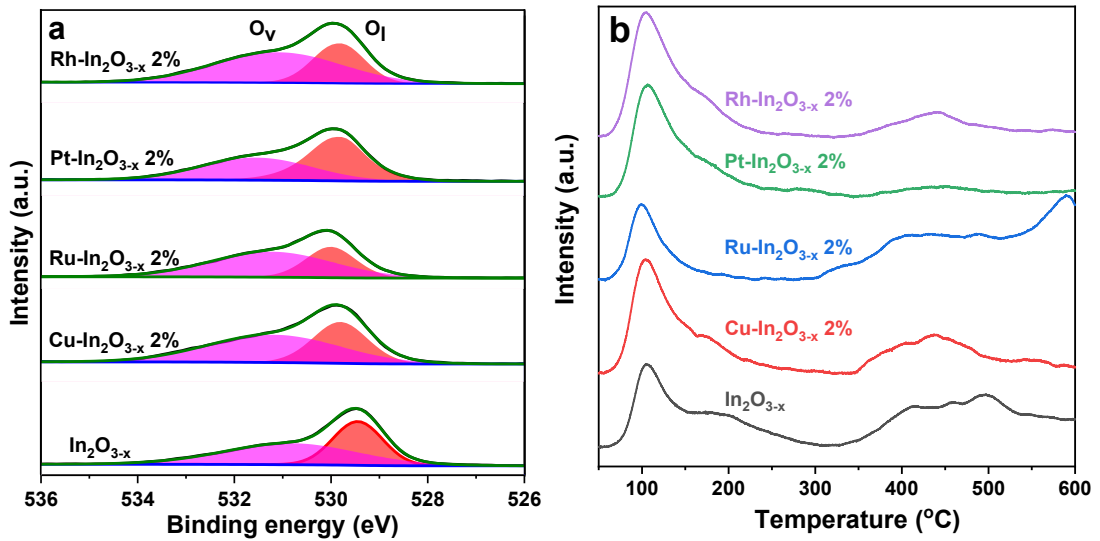
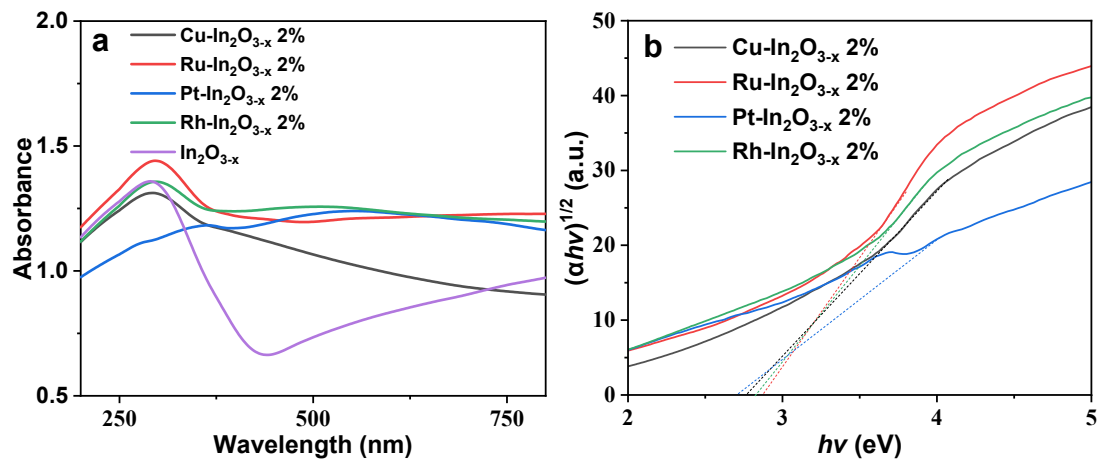


Fig. S10 (a) XPS spectra of O 1s of $\text{In}_2\text{O}_{3-x}$ doped with different metals. (b) CO_2 -TPD spectra of different metal doped $\text{In}_2\text{O}_{3-x}$.



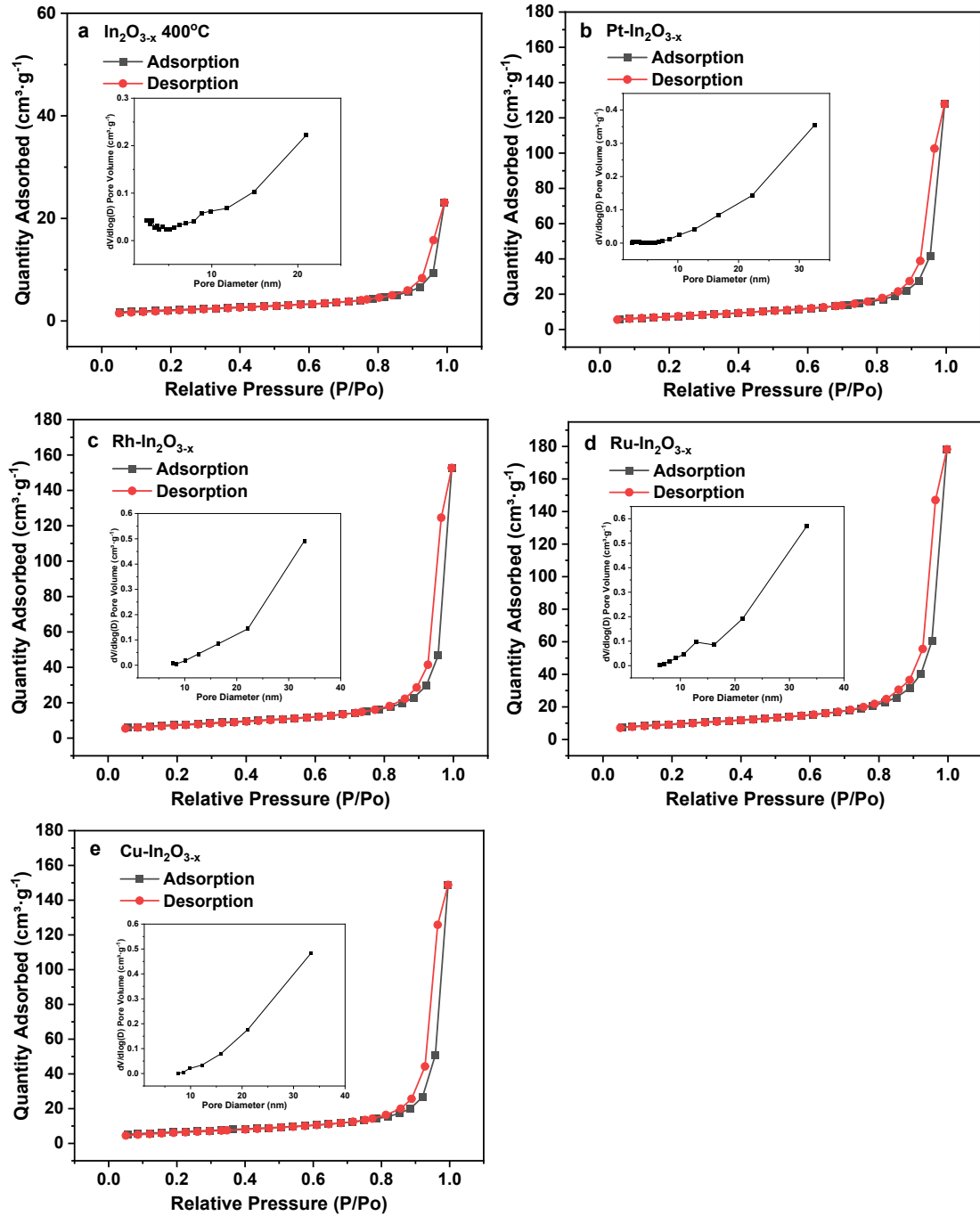


Fig. S12 N_2 adsorption desorption curves of different metal doped $\text{In}_2\text{O}_{3-\text{x}}$.

Table S1 Specific surface area, pore characteristics and loading capacity of catalysts.

Samples	S_{BET} (m ² /g)	Pore volume (cm ³ /g)	Pore diameter (nm)	Loading (%)
In ₂ O _{3-x} 400°C	7.31	0.020	11.52	0
Cu-In ₂ O _{3-x}	23.75	0.230	38.76	2.06
Ru-In ₂ O _{3-x}	33.72	0.178	32.71	1.97
Pt-In ₂ O _{3-x}	26.06	0.198	30.36	1.99
Rh-In ₂ O _{3-x}	26.82	0.236	35.23	2.09